A. Barrero-Gil, A. Sanz-Andrés

Aeroelastic effects in a traffic sign panel induced by a passing vehicle

ABSTRACT

Here, a simple theoretical model of the vehicle induced flow and its effects on traffic sign panels is presented. The model is a continuation of a previous one by Sanz-Andr´es and coworkers, now including the flexibility of the panel (and, therefore, the flow effects associated to the motion of the panel). Through the paper an aeroelastic one-degree-of-freedom model is developed and the flow effects are computed from unsteady potential theory. The influence of panel's mechanical properties (mass, damping ratio, and stiffness) in the motion induced forces are numerically analyzed.

1. Introduction

Among the structures susceptible to the action of flow are the traffic signs panels. Regular load due to the air movement of passing vehicles can result in fatigue failures as has been reported in Cali and Covert (2000). Accordingly, as aerodynamic loads eventually emerge as a significant design parameter, it is necessary to develop tools enabling the designer to estimate the effects of the moving vehicles on the signal. Unfortunately, the description of the unsteady aerodynamic forces induced by a passing vehicle is a very difficult task. Because of the size of the problem and the level of complexity, simplified mathematical models can help as a tool of modeling and prediction. In a recent article by Sanz-Andrés et al. (2004), a simple model to determine the transient aerodynamic forces induced in a traffic signal panel by the passage of a vehicle is presented. In the above mentioned model some simplifications are employed: (i) the airflow generated by the vehicle is considered incompressible and potential, where the vehicle is replaced by a source that moves at the speed of the vehicle, (ii) the characteristic timescale associated with the vehicle pass is small compared to the characteristic timescale needed to develop a boundary layer, that would lead to the buildup of a wake behind the sign, so that the model only takes into account the aerodynamic forces of non-circulatory origin, (iii) it is assumed that the vehicle is far enough from the panel, and therefore the influence of the panel on the flow around the vehicle can be neglected, and (iv) the panel is infinitely stiff. Despite its simplicity, the model provides some fairly good results when they are compared with the experimental results presented in Quinn et al. (2001), and allows to determine the role of the different geometric and kinematic variables with respect to the transient aerodynamic force on the panel (size and speed of the vehicle, vehicle distance to the signal, size and orientation of the signal). However, there are situations where the flexibility of the structure cannot be ignored without compromising the reliability of results. It seems reasonable that the next level of consideration is to take into account the flexibility of the panel and include the effect of the motion induced forces on it during the vehicle pass.

The flexibility of the cantilevered sign and signal support structures and the span of the mast arm have increased over the years (Johns and Dexter, 1998). This flexibility, combined with its inherent low mass and low damping (typically $<1\%$ of the critical damping), makes that the passage of the vehicle (either a car, a truck or a train) can induce in the sign panel (and related supports) oscillations leading to fatigue problems at the joints of the support structures. Therefore, one must take into account the aeroelastic effects in the design of the supports (or at least, one should have a reasonable theoretical background in order to asses wether such effects are negligible). The aim of this article is to include the flexibility of the panel in the model of Sanz-Andrés et al. (2004). The most important motivation is certainly of the practical consideration: from the standpoint of structural design of the panel support, one should avoid against fatigue failures, but also excessive oscillations of the panel in order to allow that the information contained in the panel be clearly displayed. Through the article we will discuss the influence of mechanical parameters (mass, damping, and stiffness) at the aerodynamics and aeroelastic forces.

The organization of the article is as follows: Section 2 presents the mathematical model and the simplifications and assumptions

on which is based. A numerical and parametric study of the relevance of the structural mass, damping, and stiffness in the aeroelastic effect is presented in Section 3. Finally, in Section 4 some conclusions that can be obtained from the model are discussed.

2. Mathematical model

To describe the interaction of a flexible structure with a flow one needs to model both the structure and the flow.

2.1. Dynamics of the panel

Here, we consider a one-degree-of-freedom approximation for the structure's dynamics, taking into account only the first deformation mode, because typically the panel is supported by a single vertical support. Thus, at a first approximation the dynamics of the panel can be considered similar to that of a slender beam (see Fig. 1). Its stiffness is represented by a linear spring, and presents a viscous linear damping. The motion of the panel is then defined by a frequency of free oscillations ω_h, a modal mass per unit length m, a dimensionless coefficient of damping ζ_h. Therefore, the displacement, h, of the panel satisfies a linear (small displacements) oscillator equation,

$$m(\ddot{h} + 2\zeta_h\omega_h\dot{h} + \omega_h^2 h) = N_h(t) + N_v(t), \tag{1}$$

where $N_h(t)$ is the aeroelastic force, per unit length, due to the bending motion (h), and $N_v(t)$ stands for the aerodynamic force due to the passing vehicle; the dot symbol stands for differentiation with respect to time t. Before the vehicle pass the panel is at rest.

2.2. Aerodynamic force induced by the vehicle passing

Here, we follow the model introduced by Sanz-Andrés et al. (2004). Let us make a brief summary. In order to develop a simple theoretical model the following assumptions are considered:

(1) The flow generated by the vehicle motion is incompressible, potential, and it is represented by a moving two-dimensional source (with the same velocity as the vehicle) whose intensity is not affected by the presence of the panel.
(2) No circulation is produced around the panel. The characteristic timescale of the vehicle pass is of order $t_p = L/U_\infty$ (L is the characteristic length of the panel ($2B$ in Fig. 1) and U_∞ is the vehicle speed) and the characteristic timescale for the development of a boundary layer on the panel is of order $t_v = L^2/v$ (being v the kinematic viscosity). Therefore, $t_p/t_v \sim \mathrm{Re}^{-1}$ (where $Re = U_\infty L/v \gg 1$ for the problem under consideration). As there is no boundary layer, circulation around the panel does not appear.
(3) The geometry of the panel is considered equivalent to a flat plate and slender enough to consider bidimensional flow around the panel (neglecting the end effects). It constitutes a barrier to the flow, so that the perpendicular component of the fluid velocity should be matched to the plate's motion.

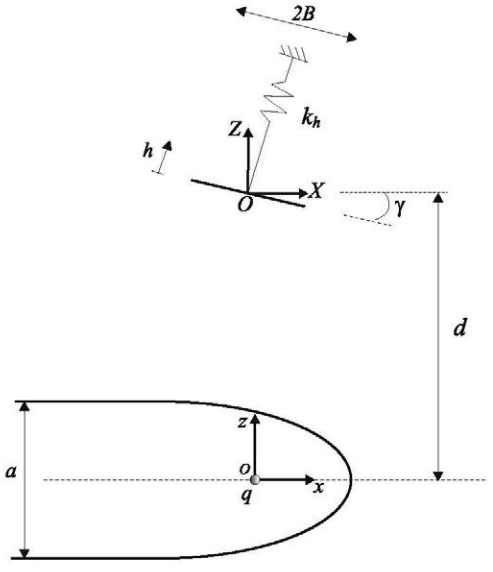

Fig. 1. Sketch of the flow around the vehicle (source) and references frames used in the analysis.

Under these assumptions it is straightforward to obtain the aerodynamic force. Using the notation defined in Fig. 1, the velocity field (u, w) in the (x, z) reference frame, fixed to the vehicle (source), is given by

$$u(x,z,t) = -U_\infty + \frac{qx}{2\pi(x^2+z^2)}, \quad w(x,z,t) = \frac{qz}{2\pi(x^2+z^2)}, \tag{2}$$

with a stagnation point located at $(q/2\pi U_\infty, 0)$. The intensity of the source is determined by the characteristic dimension of the vehicle, a, ($q = U_\infty a$).

The velocity field (U, W) on the panel can be expressed in the panel reference frame (X, W) by using the coordinate change $X = x + U_\infty t$, $Z = z + d$ [here, d is the distance in the z direction between x and X axis (distance from the center of the vehicle to the panel's center)] and the velocity composition $U = u + U_\infty$,

$$U(X,Z,t) = \frac{U_\infty a}{2\pi}\frac{X - U_\infty t}{(X - U_\infty t)^2 + (d+Z)^2}, W(X,Z,t) = \frac{U_\infty a}{2\pi}\frac{Z+d}{(X - U_\infty t)^2 + (d+Z)^2}. \tag{3}$$

Once the velocity field is known, the aerodynamic force from non-circulatory origin (normal to the plate) is equal to the apparent mass times the acceleration of the fluid (normal to the plate) evaluated at the center of the flat plate (Fung, 1955; Lighthill, 1986). For the flat plate, the apparent mass is equal to $\pi\rho B^2$ (ρ is the fluid density and B is the half-chord of the panel). Therefore, the aerodynamic force (normal to the panel) induced by the vehicle passing is given by

$$N_v(t) = \rho\pi B^2 \frac{dV_N}{dt}, \tag{4}$$

where V_N is the velocity (normal to the panel) evaluated at the center:

$$V_N = W(0,0,t)\cos\gamma + U(0,0,t)\sin\gamma, \tag{5}$$

where γ is the orientation of the panel with respect to the vehicle direction (see Fig. 1).

Evaluating $W(0,0,t)$ and $U(0,0,t)$, differentiating and introducing the dimensionless time $T = U_\infty t/d$ one arrives at the following expression for N_v:

$$N_v(T) = \rho B U_\infty^2 C_G \left(-\frac{T}{(T^2+1)^2}\cos\gamma + \frac{1}{2}\frac{T^2-1}{(T^2+1)^2}\sin\gamma \right), \tag{6}$$

where $C_G = Ba/d^2$ is a geometric factor. From Eq. (6) we can draw some conclusions: (i) the higher speed of the vehicle, the higher aerodynamically induced force at the panel and (ii) the induced aerodynamic force is proportional to the size of the vehicle, a, to the square of panel size, B, and inversely proportional to the

square distance between the panel and the vehicle, d^2. Fig. 2 shows the N_v evolution for different values of γ in a dimensionless form, $C_N(T) = N_v^{nc}(T)/\rho B U_\infty^2$, and scaled with the above mentioned geometric factor $C_G = Ba/d^2$. Note that the superscript "*nc*" remarks the non-circulatory origin of the force.

2.3. Aerodynamic force induced by the motion of the panel

Again, we only consider the effects from non-circulatory origin for the aerodynamic force induced by the motion of the panel. It is possible to check the validity of this assumption in a practical case:

(1) For typical values of the vehicle speed U_∞, the stiffness of the panel, ω_h, and distance between the panel and the vehicle, d, the characteristic convective time of the flow around the panel is of the order $t_c \sim 8\pi Bd/(U_\infty a)$ is large compared to the characteristic time of panel's oscillations, of the order $t_o \sim \omega_h^{-1}$. Note that to estimate t_c is necessary to obtain the maximum tangential velocity induced by the vehicle pass in center of the panel. For example, taking $\gamma = 0$, from Eq. (3) it is straightforward to get that

$$U(0,0,T) = -\frac{U_\infty a}{2\pi d}\frac{T}{T^2+1}, \quad \frac{dU(0,0,T)}{dT} = -\frac{U_\infty a}{2\pi d}\left(\frac{1}{T^2+1} - \frac{2T^2}{(T^2+1)^2}\right),$$

and therefore

$$V_{T_{max}} = U(0,0,-1) = \frac{U_\infty a}{4\pi d}.$$

As a practical example, taking $U_\infty = 30\,\mathrm{m/s}$, $\omega_h = 15\,\mathrm{s}^{-1}$, $d = 4\,\mathrm{m}$, $B/a = 0.25$ one gets $t_c = 4\pi/15 \sim 1\mathrm{s}$, and $t_o = 1/15 \sim 10^{-1}\,\mathrm{s}$.

(2) The oscillatory Reynolds number ($Re_\omega = 2\omega_h \varepsilon B^2/\nu$, where εB is the amplitude of the oscillation) is large compared with the unity, so that viscosity effects can be neglected. Indeed, there is no need to consider compressibility effects ($\omega_h L/c \gg 1$, where c is the sound speed).

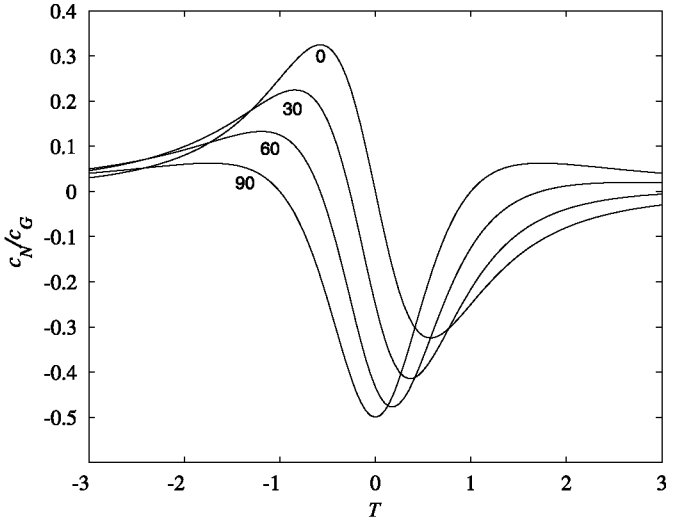

Fig. 2. Aerodynamic force coefficient [normal to the plate (panel)] due to the vehicle passing (defined as $C_N(T) = N_v(T)/\rho\pi BU_\infty^2$) normalized with a geometrical factor ($C_G = Ba/\pi d^2$), as a function of the dimensionless time $T = U_\infty t/d$. Numbers stand for the panel's orientation, γ, in degrees, with regard to the vehicle's line of motion.

Under these assumptions, the aerodynamic force is given by

$$N_h^{nc}(t) = -\rho\pi B^2 \ddot{h}, \tag{7}$$

where the negative sign denotes that the force is in the opposite direction to the movement of the panel; the dot denotes differentiation with respect to time t, and the superscript stress the non-circulatory origin of the force. Introducing the dimensionless time T, one gets

$$N_h^{nc}(T) = -\rho\pi B^2\left(\frac{U_\infty^2}{d^2}h''\right), \tag{8}$$

where the comma indicates differentiation with respect to dimensionless time T. Obviously this result will be valid as long as oscillation amplitudes are so small that the flow does not separate from the oscillating panel. Some experiments (Ackerman and Arbhabhirama, 1964) show that the amplitude must be lower than 10% (referred to the length of the panel, that is $h/(2B) < 0.1$) to avoid flow separation.

2.4. Dimensionless equation for the panel's dynamics

As a result of substituting Eqs. (6) and (8) in Eq. (1), introducing a dimensionless displacement $\eta = h/2B$, and time T, the equation of the panel's dynamics in a dimensionless form is obtained,

$$U_r^2\eta'' + 2\zeta_h U_r \eta' + \eta = \pi\mu_B U_r^2 \left(-\eta'' - \frac{a}{2\pi B}\frac{T}{(T^2+1)^2}\cos\gamma + \frac{a}{4\pi B}\frac{T^2-1}{(T^2+1)^2}\sin\gamma\right). \tag{9}$$

In this equation $\mu_B = \rho B^2/m$ is the mass ratio and $U_r = U_\infty/(\omega_h d)$ is a reduced velocity.

3. Aeroelastic effects. Influence of the panel's mechanical properties

A parametric study has been carried out to investigate the separated effects of mass ratio ($\mu_B = \rho B^2/m$), damping (ζ_h), and stiffness, which are most interesting from the standpoint of practical reasons (they can be modified by the designer). Observe that stiffness is considered through its role on the reduced velocity, $U_r = U_\infty/(\omega_h d)$. In all cases the strategy is the same: a set of parameters are fixed (baseline configuration) except those whose influence is under study. To present the results a dimensionless force coefficient is defined as follows:

$$c_N^* = -\eta'' - \frac{a}{2\pi B}\frac{T}{(T^2+1)^2}\cos\gamma + \frac{a}{4\pi B}\frac{T^2-1}{(T^2+1)^2}\sin\gamma. \tag{10}$$

In all cases, the equation of the dynamics (Eq. (9) considering that the panel is initially at rest) has been numerically solved by means of a Runge–Kutta scheme. For comparison purposes, we will plot c_N^* in both conditions: considering the flexibility of the panel, and computed for the case when the panel is assumed rigid.

3.1. Effect of the mass ratio

Fig. 3 illustrates a plot of c_N^* for two different values of mass ratio. Damping, stiffness, geometry and kinematic parameter has been kept fixed: $\zeta_h = 0.01$, $U_r = 0.5$, $a/2B = 2$, $\gamma = 0^\circ$.

Observe in Fig. 3. that the aeroelastic effect is more intense for lower values of mass ratio, case (a). In particular, for $\mu_B = 0.25$ there has been an increase in c_N^* (peak to peak) of about 20%. Moreover, there is a slight change in the history of c_N^*: when the

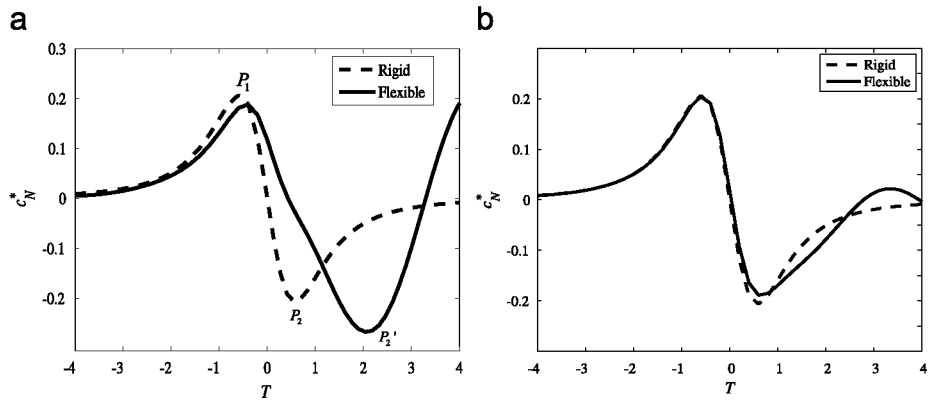

Fig. 3. Influence of the mass ratio in the aeroelastic effect. Aerodynamic force coefficient c_N^* with and without flexibility in the panel, as a function of dimensionless time $T = U_\infty t/d$: (a) $\mu_B = 0.25$ and (b) $\mu_B = 0.025$.

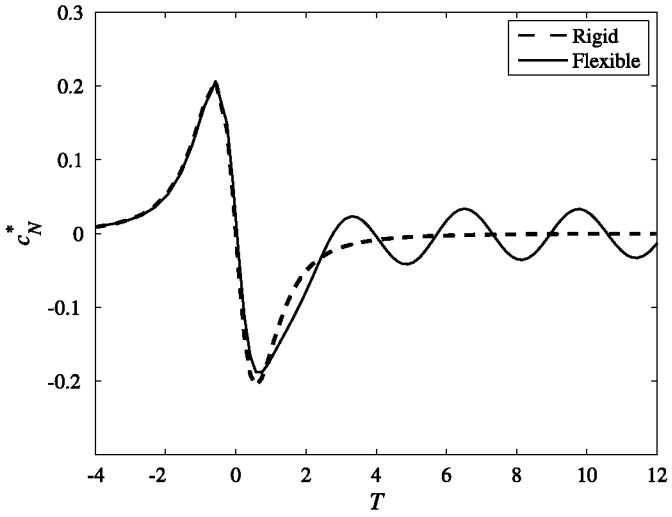

Fig. 4. Fatigue effect. Aerodynamic force coefficient c_N^* with and without flexibility in the panel, as a function of dimensionless time $T = U_\infty t/d$: (a) $\mu_B = 0.25$ and (b) $\mu_B = 0.025$.

flexibility is considered, the second peak (P_2' as has been denoted in Fig. 3) has shifted to the right (the initial load cycle is longer).

Another consequence is that flexibility produces more than one cycle of oscillation (and hence load cycle) on the panel, as shown in Fig. 4. The vehicle passing not only implies an initial intense overpressure and subsequent depression (load cycle), but involves several trailing loads cycles as the panel is still oscillating after the vehicle passing until oscillations are damped out, due to friction effects. With regard to this point, mass ratio has opposite effects. For low values of μ_B the initial secondary load cycles are more intense but they are rapidly damped out. Conversely, when μ_B is high a lot of small secondary load cycles appears. Obviously, this is an important point in the design panel, because of its contribution to fatigue effects.

3.2. Effect of reduced velocity (stiffness of the panel)

Fig. 5 shows a plot of c_N^* for two different values of U_r (note that it is dependent on ω_h, as well as d and U_∞). Mass ratio, damping, geometry and kinematic parameter are fixed: $\mu_B = 0.1$, $\zeta_h = 0.01$, $a/2B = 2$, $\gamma = 0^\circ$. From the figure one can observe that the aeroelastic effect is more intense for higher values of U_r (lower stiffness). For the case when $U_r = 0.25$ there has been a peak pulling into the road ($c_N^* < 0$) of 20% approximately. When $U_r = 0.1$ the aeroelastic effect is very small: barely a slight oscillation superimposed on static c_N^* curve. In both cases, period of the first load cycle is approximately the same than that of the rigid panel.

3.3. Effect of damping

Fig. 6 shows a plot of c_N^* for two different values of the critical damping coefficient ζ_h. Mass ratio, stiffness, geometry and kinematic parameter are fixed: $\mu_B = 0.1$, $U_r = 0.2$, $a/2B = 2$, $\gamma = 0^\circ$. The peak pulling into the road ($c_N^* < 0$) is approximately the same in both cases. However, from the figure one can deduce that structural damping has a beneficial effect, case (a), especially to mitigate possible fatigue effects.

3.4. Effect of the orientation of the panel (γ)

For practical purposes it is interesting to present as example a plot of c_N^* when $\gamma = 90^\circ$ (the panel is perpendicular with respect to the road). Fig. 7 shows the results for $\mu_B = 0.1$, $U_r = 0.2$, $a/2B = 2$, $\zeta_h = 0.01$. Observe that the flexibility of the panel induces a more intense pulling effect (centered approximately at $T = 0$, when the vehicle is just passing ahead the panel), as well as the emergence of secondary load cycles.

4. Conclusions

The investigation on aerodynamic and fluid motion falls naturally in two parts: (i) the experimental or practical side, and (ii) the theoretical side which attempts to explain why experimental results change as they do. Thus the practical and theoretical sides supplement one another. The aim of this article has been to develop a very simple theoretical model to take into account the aeroelastic effects in the response of traffic sign panels under vehicle passing (or to establish when this effects becomes of secondary order). The model is based on unsteady potential flow and only non-circulatory flow effects are considered. The model is valid when $t_o \sim t_p << t_v$ where, t_o, t_p, and t_v are, respectively, the characteristic time of oscillation of the panel, vehicle pass time and viscous time. This requirement can be fulfilled in practical situations as shown in the paper.

Unfortunately there is no experimental data to test the theoretical model developed, but the point made clear here is that flexibility must be take into account for low values of mass, damping, and stiffness. On the other hand, experiments carried

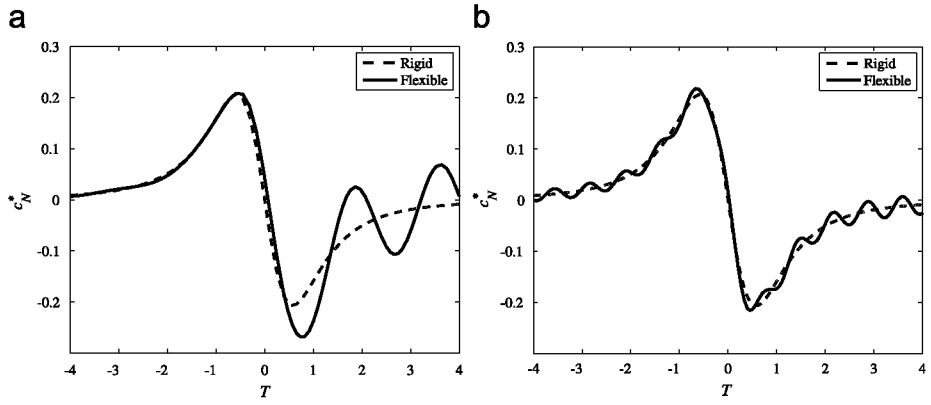

Fig. 5. Influence of the stiffness in the aeroelastic effect. Aerodynamic force coefficient c_N^* with and without flexibility in the panel, as a function of dimensionless time $T = U_\infty t/d$: (a) $U_r = 0.25$ and (b) $U_r = 0.1$.

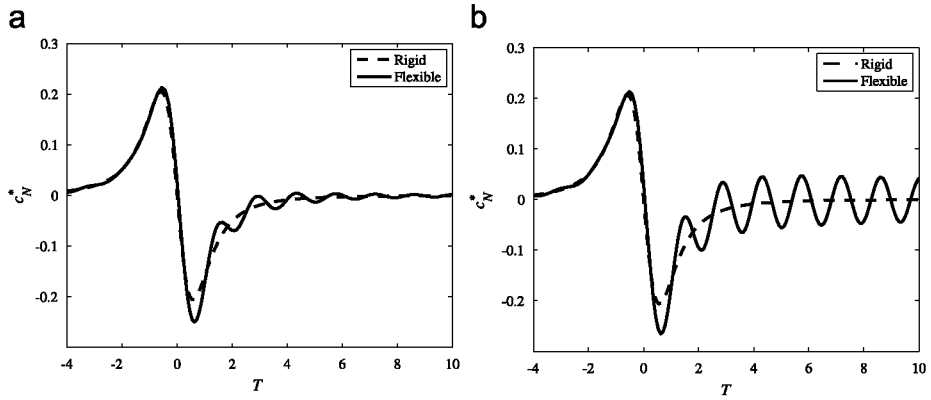

Fig. 6. Influence of damping in the aeroelastic effect. Aerodynamic force coefficient c_N^* with and without flexibility in the panel, as a function of dimensionless time $T = U_\infty t/d$: (a) $\zeta_h = 0.1$ and (b) $\zeta_h = 0.01$.

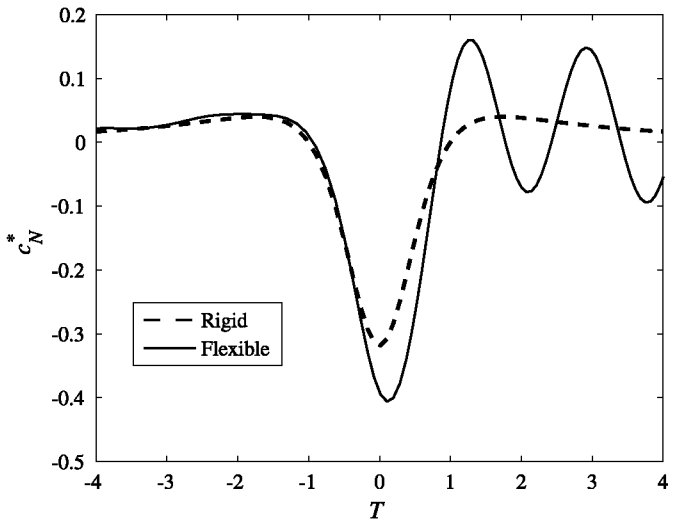

Fig. 7. Aerodynamic force coefficient c_N^* with and without flexibility in the panel, as a function of dimensionless time $T = U_\infty t/d$ when $\gamma = 90^\circ$.

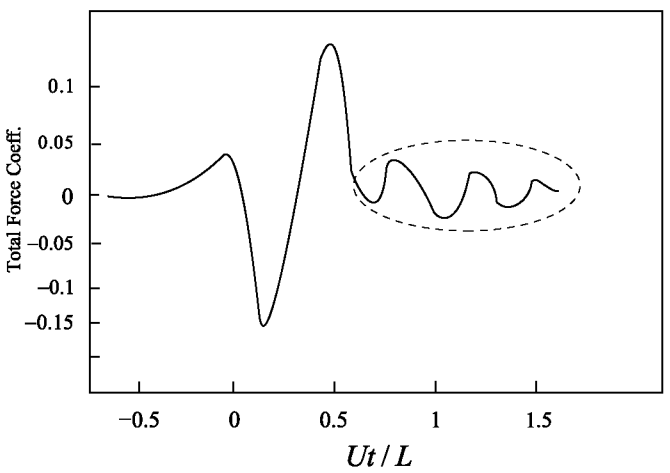

Fig. 8. Experimental dependence of total force coefficient with time measured by Cali and Covert (paper's figure number 7).

out by Cali and Covert (2000) show that the variation of force coefficient with time (see Fig. 8) presents several peaks and zero crossings. Those investigators refers that the secondary load cycles can be due to wake effects of the vehicle. Obviously, this is a possibility, but we believe that the analysis presented here shows that a second possibility needs to be considered: the flexibility of the panel in the experimental set-up. It would be very useful to consider the elastic properties in future experimental tests in order to elucidate this question. Moreover, the analysis shows that increasing structural damping is an effective way to mitigate the above mentioned secondary load cycles.

References

Ackerman, N.L., Arbhabhirama, A., 1964. Viscous and boundary effects on virtual mass. ASCE Journal Engineering Mechanics Division 90 (EM4), 123.

Cali, P.M., Covert, E.E., 2000. Experimental measurements of loads on a overhead highway sign structure by vehicle-induced gusts. Journal of Wind Engineering and Industrial Aerodynamics 84, 87–100.
Fung, Y.C., 1955. An Introduction to the Theory of Aeroelasticity. Dover, New York.
Johns, K.W., Dexter, R.J., 1998. The development of fatigue design load ranges for cantilevered sign and signal support structures. Journal of Wind Engineering and Industrial Aerodynamics 77–78, 315–326.

Lighthill, J., 1986. An Informal Introduction to Theoretical Fluid Mechanics. Oxford University Press, New York.
Quinn, A., Baker, C.J., Wright, N.G., 2001. Wind and vehicle induced forces on flat plates. Part 2: vehicle induced force. Journal of Wind Engineering and Industrial Aerodynamics 89, 831–847.
Sanz-Andrés, A., Santiago-Prowald, J., Baker, C., Quinn, A., 2004. Vehicle-induced loads on traffic sign panels. Journal of Wind Engineering and Industrial Aerodynamics 91, 925–942.